# Cylinder air/fuel ratio estimation using net heat release data

Tunestål, Per; Hedrick, J. Karl

*Published in:*
Control Engineering Practice

*DOI:*
10.1016/S0967-0661(02)00045-X

2003

Available online at www.sciencedirect.com
SCIENCE DIRECT®
PERGAMON
Control Engineering Practice 11 (2003) 311–318
CONTROL ENGINEERING PRACTICE
www.elsevier.com/locate/conengprac

# Cylinder air/fuel ratio estimation using net heat release data

Per Tunestål[a], J. Karl Hedrick[b,*]

[a] Lund Institute of Technology, Div. Combustion Engines, P.O. Box 118, SE-221 00 Lund, Sweden
[b] Department of Mechanical Engineering, University of California, Berkeley, 6189 Etcheverry Hall, Berkeley, CA 94720-1740, USA

Received 26 October 2001; accepted 14 December 2001

**Abstract**

An estimation model which uses the net heat release profile for estimating the cylinder air/fuel ratio of a spark ignition engine is developed. The net heat release profile is computed from the cylinder pressure trace and quantifies the conversion of chemical energy of the reactants in the charge into thermal energy. The net heat release profile does not take heat- or mass transfer into account. Cycle-averaged air/fuel ratio estimates over a range of engine speeds and loads show an RMS error of 4.1% compared to measurements in the exhaust. 

*Keywords:* Engine control; Engine modelling; Pressure; Least-squares estimation; Least-squares identification

## 1. Introduction

Increasingly high demands on pollutant control on automotive engines have been pushing the level of sophistication of engine control modules (ECM) higher and higher for more than twenty years from now. The three-way catalytic converter, which completely dominates the after treatment of exhaust gases from automotive spark ignition (SI) Engines, mandates that the air/fuel ratio (AFR) is kept in a very narrow band around stoichiometric. A modern ECM handles this task very well under steady-state conditions by estimating the air/fuel ratio using an oxygen sensor in the exhaust gas stream. The control problem becomes more difficult during transient operation, though. The inherent time delay in the feedback system due to the placement of the oxygen sensor in the exhaust imposes a bandwidth limitation on the closed-loop system. This bandwidth limitation will result in AFR excursions during fast transients, which in turn will result in increased pollutant emissions.

A sensor inside the combustion chamber providing information that replaces the oxygen sensor signal, would drastically reduce the time delay in the feedback system, and could consequently reduce the AFR excursions during fast transients. In this paper, cylinder pressure is used as a source of feedback. Many approaches in how best to utilize cylinder pressure feedback have been proposed (Powell, 1993; Wibberley & Clark, 1989; Pestana, 1989). Most approaches that have previously been proposed require statistics over a large number of cycles, which defeats the purpose of trying to reduce the time delay in the feedback system. For example, it has been found that, using the indicated mean effective pressure (imep), up to 300 engine cycles are required to achieve acceptable repeatability and accuracy (Brunt & Emtage, 1996). Tunestål, Lee, Wilcutts, and Hedrick (2000) presents an ad hoc attempt at higher bandwidth feedback using cylinder pressure.

This paper develops a method to estimate the AFR in an SI engine from cylinder pressure measurements. The method is developed from a well-established empirical model for the dependence of laminar flame speed on temperature, pressure, and AFR, and relates this model to the heat-release rate during the rapid burn phase, which is obtained from the cylinder-pressure-based net heat release profile.

Since the actual flame speed in an SI engine depends on the turbulence intensity, a turbulence model also has to be included. This model includes a simple turbulence model implicitly, by assuming that the turbulence intensity is a function of engine speed (Heywood, 1988).

An AFR estimator which is able to estimate cylinder AFR from cylinder pressure measurements over a wide range of operating points is developed. The variance of

*Corresponding author. Tel.: +1-510-642-0870; fax: +1-510-642-6163.
*E-mail addresses:* per.tunestal@vok.lth.se (P. Tunestål), khedrick@me.berkeley.edu (J.K. Hedrick).

0967-0661/02/$ - see front matter 
PII: S0967-0661(02)00045-X

an individual cycle estimate is very high due to the random nature of the amount of residual gas in the cylinder, as well as the turbulent flow field which will cause the flame development to be different from cycle to cycle. Cycle-averaged AFR estimates show an RMS error of only 4.1% though. The identification and validation are based on experiments performed at the University of California, Berkeley. The experimental setup is essentially the same as in Tunestål, Wilcutts, Lee, and Hedrick (1999), and the work is based on Tunestål (2000).

## 2. Review of the concepts of flame and flame speed

The following section is a review of the concepts of flame and flame speed, and is included for completeness. The presentation is largely based on Heywood (1988).

### 2.1. Definition of flame

A flame is a combustion reaction which propagates subsonically through space. For motion of the reaction zone to be well-defined, it is assumed that the thickness of the reaction zone is small compared to the dimensions of the space it is confined to. Propagation of the reaction zone refers to its motion relative to the unburned gas ahead of it, and thus a propagating flame can very well be stationary with respect to the observer.

Two different classes of flames can be distinguished based on where the mixing of fuel and oxidizer (air) takes place. If fuel and oxidizer are uniformly mixed when entering the reaction zone, a *premixed* flame results. A *diffusion* flame results if fuel and oxidizer have to mix as the reaction is taking place. Similarly, flames can be characterized based on the gas flow characteristics in the reaction zone. Flames can be either *laminar* (stream lined flow), or *turbulent* (vortex motion). Flames can be classified as *unsteady* or *steady* depending on whether their overall motion or structure change with time or not. Finally, the initial phase of the fuel, when it enters the reaction zone can be used for classification of the flame. It can be either *solid*, *liquid* or *gaseous*.

The flame in an SI engine is premixed, turbulent, and unsteady, and the fuel is gaseous when it enters the reaction zone.

### 2.2. Laminar and turbulent flame speed

The laminar flame speed is defined as the velocity, relative and normal to the flame front, with which the unburned gas moves into the front and is converted into products under laminar flow conditions (see Fig. 1). This definition originates from experiments with burners, where the flame is stationary, the unburned gas moves into the flame, and the burned gas moves out of and away from the flame. The density of the burned gas is, in general, lower than the density of the unburned gas, and consequently the burned gas will have a higher velocity than the unburned gas.

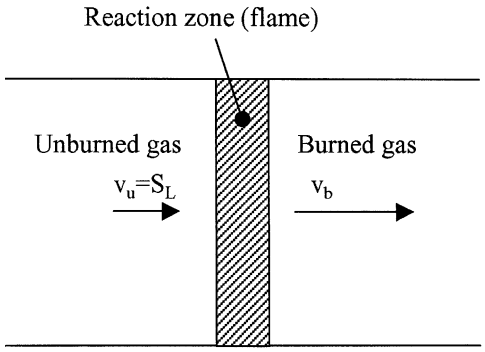


Fig. 1. Illustration of a stationary laminar flame with unburned gas entering the reaction zone at the laminar flame speed, $S_L = v_u$, and leaving the reaction zone at a velocity, $v_b > v_u$.

A situation more relevant to engines, is that the unburned gas is stationary, and the reaction zone propagates through the gas. In this case the laminar flame speed is actually the speed at which the flame front propagates (see Fig. 2). The laminar flame speed under engine pressure and temperature is of the order 0.5 m/s. In reality, the unburned gas in an engine actually moves away from the flame front, due to the expansion of the burned gas and compression of the unburned gas.

One might be tempted to claim that the laminar flame speed is of limited interest for internal combustion engines, since the flow conditions in any practical engine are highly turbulent. It turns out however, that one important way of modeling the turbulent flame development (see Section 2.2) which actually takes place in an internal combustion engine, includes the laminar flame concept as a submodel.

The presence of turbulence aids in propagating the flame, and since the local gas velocities due to turbulence can be significantly higher than the laminar flame speed, turbulence can drastically increase the actual speed with

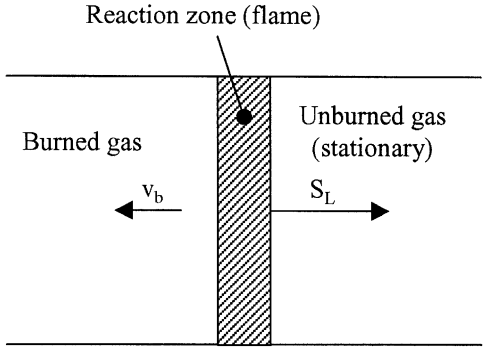


Fig. 2. Illustration of a propagating laminar flame. The flame front moves at the laminar flame speed, $S_L$, into the stationary unburned gas. Due to the expansion, the burned gas is pushed backwards out of the reaction zone at a velocity, $v_b$.

which the reaction zone propagates. This speed is called the turbulent flame speed. Groff and Matekunas (1980) indicates that the turbulent flame speed is proportional to the laminar flame speed, and a factor which increases monotonically with the turbulence intensity.

## 3. Flame speed models

### 3.1. A laminar flame speed model

The laminar flame speed of a premixed gasoline/air flame increases monotonically with temperature, decreases monotonically with pressure, and peaks for equivalence ratios slightly rich of stoichiometric. This behavior can be modeled empirically by

$$S_L = S_{L,0}\left(\frac{T_u}{T_0}\right)^{\beta}\left(\frac{p}{p_0}\right)^{\mu}, \tag{1}$$

where $S_{L,0}$ is the laminar flame speed at $T_0 = 298$ K and $p_0 = 1$ atm. $T_u$ represents the temperature of the unburned gas ahead of the flame, and $p$ is the pressure. The parameters $\beta$ and $\mu$ are empirical model parameters and depend slightly on the equivalence ratio.

The laminar flame speed at normal pressure and temperature, $S_{L,0}$ can be modeled by

$$S_{L,0} = B_m + B_\phi(\phi - \phi_m)^2. \tag{2}$$

Here, $B_m$ represents the maximum flame speed attained at equivalence ratio $\phi_m$, and $B_\phi$ quantifies the dependence of flame speed on equivalence ratio. The following values were experimentally identified by Metgalchi and Keck (1982) for the laminar flame speed of a gasoline/air flame:

$$\phi_m = 1.21,$$
$$B_m = 0.305 \text{ m/s},$$
$$B_\phi = -0.549 \text{ m/s}.$$

The range of equivalence ratios relevant for an SI engine intended for stoichiometric operation is roughly $[0.9, 1.1]$, which means that the laminar flame speed varies approximately $\pm 8\%$ relative to the stoichiometric value.

### 3.2. Modeling the turbulent flame speed

It is discussed in Heywood (1988) that the rapid burn angle $\Delta\alpha_b$, i.e. the crank angle interval between 10% and 90% heat release, increases only slightly with engine speed. This implies that the turbulence intensity increases with engine speed, which causes an increase in the flame speed. Measurements in Hires, Tabaczynski, and Novak (1978) indicate that the rapid burn angle, with inlet pressure and equivalence ratio constant, follows approximately a power law with respect to engine speed, $N$, according to

$$\Delta\alpha_b \sim N^{0.37}. \tag{3}$$

Since the way the turbulent flow characteristics change with engine speed depends on the engine geometry, the exponent in the previous equation is considered as an unknown, $\eta$, which has to be determined from experiments. Thus,

$$\Delta\alpha_b = kN^{\eta} \tag{4}$$

for some constant $k$.

The time it takes for the flame to propagate from the spark gap to the farthest end of the combustion chamber can be expressed as

$$\Delta t_b = \frac{sB}{u_f}, \tag{5}$$

where $B$ is the cylinder bore, $s$ is a factor which depends on the location of the spark gap, and $u_f$ is the flame speed. A simple relationship based on the engine speed relates $\Delta t_b$ and $\Delta\alpha_b$,

$$\Delta\alpha_b = \frac{\mathrm{d}\alpha}{\mathrm{d}t}\Delta t_b = \frac{2\pi N}{60}\Delta t_b. \tag{6}$$

Thus, the flame speed can be expressed in terms of the rapid burn angle,

$$u_f = \frac{2\pi sBN}{60\Delta\alpha_b}. \tag{7}$$

Combining (4) and (7) yields

$$u_f = u_0\left(\frac{N}{N_0}\right)^{1-\eta}, \tag{8}$$

where

$$u_0 = \frac{2\pi sBN_0^{1-\eta}}{60k} \tag{9}$$

and $N_0$ is some arbitrary engine speed. It should be noted here that $u_0$ will depend on equivalence ratio, pressure, and temperature in the same way as the laminar flame speed, according to (2). Now, assuming that $\phi$ is close enough to $\phi_m$,

$$u_0 = u_{00}\left(\frac{T_u}{T_0}\right)^{\beta}\left(\frac{p}{p_0}\right)^{\mu}. \tag{10}$$

## 4. Incorporating the cylinder-pressure-based heat release into the flame speed models

### 4.1. Relating burn rate to flame speed

A common simplification when modeling flame propagation in a spark-ignition engine is to assume that the flame front propagates spherically outward from the spark plug. Due to the finite nature of the combustion chamber, the flame-front area quickly assumes a nearly constant value (see Fig. 3), $A_f$. Thus, the enflamed

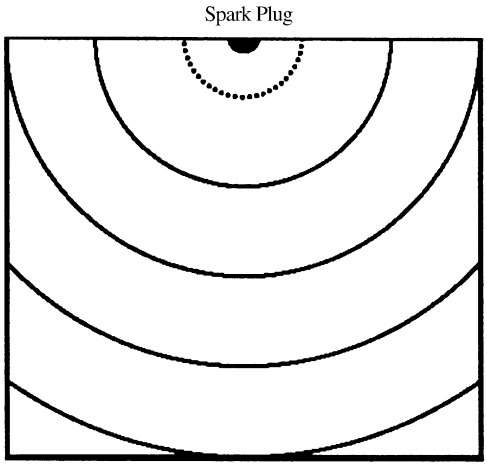


Fig. 3. Two-dimensional illustration of flame propagation from the spark plug. The circle segments represent the flame front as it propagates radially outward from the spark gap. All flame fronts marked with solid lines are essentially of equal length.

volume will grow according to

$$\frac{\mathrm{d}V_f}{\mathrm{d}t} = A_f u_f. \tag{11}$$

The rate at which fuel is consumed can now be expressed using (11) and the ideal gas law.

$$\frac{\mathrm{d}m_f}{\mathrm{d}t} = \frac{m_f}{V}\frac{\mathrm{d}V_f}{\mathrm{d}t} = \frac{m_f}{m_a}\frac{m_a}{V}\frac{\mathrm{d}V_f}{\mathrm{d}t} \approx \frac{1}{\mathrm{AFR}}\frac{p}{RT}A_f u_f. \tag{12}$$

An approximation has been made in the application of the ideal gas law. The fuel mass has been neglected in assuming

$$pV = m_a RT. \tag{13}$$

Since the AFR in a gasoline engine is nominally 14.7, this is a reasonable approximation.

The angular velocity, $\omega_e$, of the engine relates crank-angle derivatives and time derivatives according to

$$\frac{\mathrm{d}m_f}{\mathrm{d}\alpha} = \frac{\mathrm{d}m_f}{\mathrm{d}t}\Big/\omega_e. \tag{14}$$

Introducing $N$ as the engine speed in revolutions per minute yields

$$\frac{\mathrm{d}m_f}{\mathrm{d}\alpha} = \frac{60 A_f u_f p}{2\pi N\,\mathrm{AFR}\,RT}. \tag{15}$$

Using (8) for the flame speed, (15) can be rewritten as

$$\frac{\mathrm{d}m_f}{\mathrm{d}\alpha} = \frac{60 A_f u_0 p N^{-\eta}}{2\pi N_0^{1-\eta}\,\mathrm{AFR}\,RT}. \tag{16}$$

Using (10) and consolidating the multiplicative constant, an expression for the burn rate as a function of pressure, temperature, and engine speed is obtained

$$\frac{\mathrm{d}m_f}{\mathrm{d}\alpha} = b p^{1+\mu} T^{\beta-1} N^{-\eta}\,\mathrm{AFR}^{-1}, \tag{17}$$

for some constant $b$.

### 4.2. Relating burn rate to average heat release rate

During the rapid burn phase of the cycle, the heat-release rate is essentially constant in the crank-angle domain. Thus, during the bulk of the combustion event, the heat-release rate can approximately be expressed as

$$\frac{\mathrm{d}Q_{ch}}{\mathrm{d}\alpha} \approx \frac{Q_{tot}}{\Delta\alpha_b}. \tag{18}$$

The chemical energy released when combusting a unit mass of fuel with air is the lower heating value, $Q_{LHV}$. Thus, the rate of fuel conversion can be expressed as

$$\frac{\Delta m_f}{\Delta\alpha} = \frac{1}{Q_{LHV}}\frac{Q_{tot}}{\Delta\alpha_b}. \tag{19}$$

Combining the two expressions for the burn rate, (17), provides an equation from which the AFR can be determined. The pressure and temperature at the start of combustion are determined by a compression polytrope from the inlet pressure and temperature. Thus, the inlet pressure and temperature, $p_0$, $T_0$, can be used according to

$$b p_0^{1+\mu} T_0^{\beta-1} N^{-\eta}\,\mathrm{AFR}^{-1} = \frac{1}{Q_{LHV}}\frac{Q_{tot}}{\Delta\alpha_b}. \tag{20}$$

Isolating AFR yields

$$\mathrm{AFR} = b Q_{LHV}\frac{\Delta\alpha_b}{Q_{tot}} p_0^{1+\mu} T_0^{\beta-1} N^{-\eta}. \tag{21}$$

So, with $c = bQ_{LHV}$,

$$\mathrm{AFR} = c\frac{\Delta\alpha_b}{Q_{tot}} p_0^{1+\mu} T_0^{\beta-1} N^{-\eta}, \tag{22}$$

where $c$, $\mu$, $\beta$, and $\eta$ are unknown constants, which have to be determined from experiments.

## 5. Identification of model parameters

### 5.1. Identification method

The experimental setup used for this work does not allow control of the intake air temperature, and thus only the dependence of AFR on burn rate, pressure, and engine speed are investigated. In the identification experiments, the coolant temperature is held constant, in order to prevent any influence from this temperature.

In order to identify the unknown parameters of (22), it is rewritten by taking logarithms

$$\ln\left(\frac{\mathrm{AFR}}{\Delta\alpha_b/Q_{tot}}\right) = \ln(cT_0^{\beta-1}) + (1+\mu)\ln p_0 + (-\eta)\ln N. \tag{23}$$

Define the parameter vector

$$\theta = \begin{pmatrix} \ln(cT_0^{\beta-1}) \\ 1+\mu \\ -\eta \end{pmatrix}, \tag{24}$$

the vector of regressors

$$\varphi = (1 \ln\ p_0\ \ln\ N), \tag{25}$$

and the output

$$y = \ln\left(\frac{\mathrm{AFR}}{\Delta\alpha_b/Q_{tot}}\right). \tag{26}$$

An estimate for $\theta$, $\hat{\theta}$, can now be calculated from $n$ cycles of measurements using least-squares regression, see Johansson (1993).

The parameter estimate obtained from the linear least-squares solution above minimizes the sum of squared residuals of the form

$$r_{\ln} = \ln(\hat{\mathrm{AFR}}) - \ln(\mathrm{AFR}) = \ln\left(\frac{\hat{\mathrm{AFR}}}{\mathrm{AFR}}\right). \tag{27}$$

This is not the same however, as minimizing the sum of squares of the estimation error

$$r = \hat{\mathrm{AFR}} - \mathrm{AFR}. \tag{28}$$

Since a ratio is being estimated though (the ratio of air mass to fuel mass in the cylinder), it makes more sense to minimize (27).

### 5.2. Identification experiments

When applying experimental data to the estimation method described above, it has to be decided which pressure to use in the regression vector (25). Here, $p_0$ is selected as the cylinder pressure at a fixed crank angle during the compression stroke. This pressure, because of the polytropic compression relation (Tunestål, 2000), scales with the pressure at the onset of combustion.

The experiments were carried out as steady-state experiments at different loads, engine speeds, and AFR. Each steady-state experiment lasts for approximately 10 s. For each of these experiments, the mean exhaust AFR is selected as the "true" AFR for all the cycles of that experiment. The reason for this is that the true AFR for the individual cylinder cycles cannot be singled out when using exhaust AFR measurements.

Fig. 4 shows the result of the least-squares fit applied to the identification data. The variance of the estimate is quite large, and requires some kind of filtering in order to be of practical use. Fig. 5 shows the residuals for the same data.

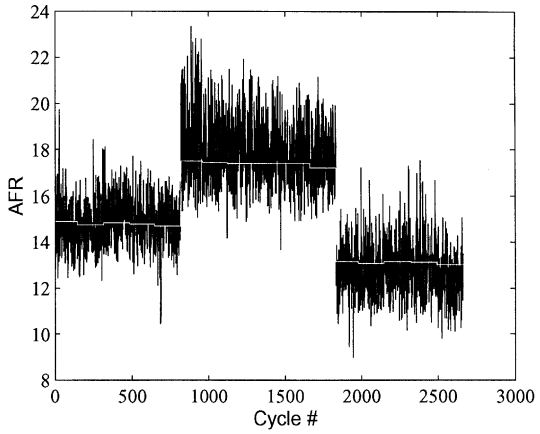


Fig. 4. Estimated AFR (black line) and measured AFR (white line).

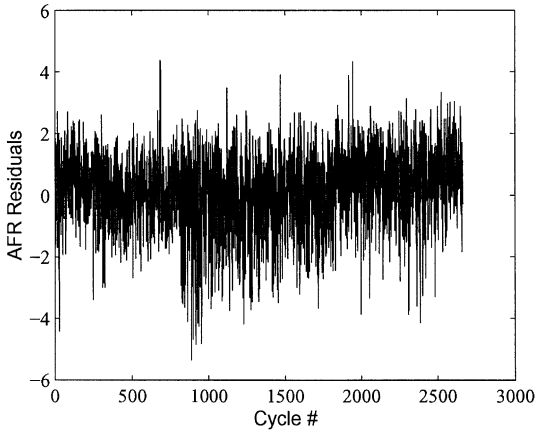


Fig. 5. Residuals of least-squares AFR fit.

## 6. Model validation

The presented model for AFR estimation was validated by conducting similar experiments as the ones used for the identification. The result of these measurements in terms of estimated AFR versus measured exhaust AFR are shown in Fig. 6.

The plot shows that except for at very lean operating points ($\mathrm{AFR} \geqslant 18$), the estimator performs well. For the leanest operating points, the estimator tends to overestimate the AFR. This is caused by the fact that the engine is operating near its lean limit. At the lean limit, combustion is either too slow to finish before the exhaust valve opens, or the gas temperature is so low that the flame extinguishes before it reaches the far cylinder wall. For both these cases, the result is that not all of the fuel is combusted, and thus the heat release is significantly lower. Since the estimated AFR is inversely proportional to the heat release, this will result in an overestimated AFR.

Fig. 7 shows the heat release for 248 consecutive cycles with an air/fuel ratio of 18.1, and it is easily seen

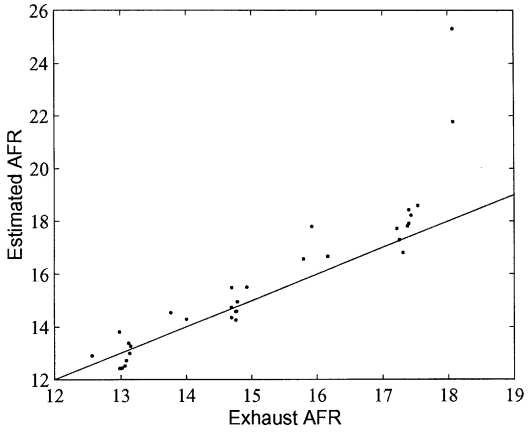


Fig. 6. Cycle-averaged (10 s) estimated AFR plotted versus measured exhaust AFR. Experiments conducted at a range of engine speeds, loads, and Air/Fuel Ratios. The RMS error in the estimate is 4% when excluding the two estimates at the lean limit (AFR $\geqslant$ 18).

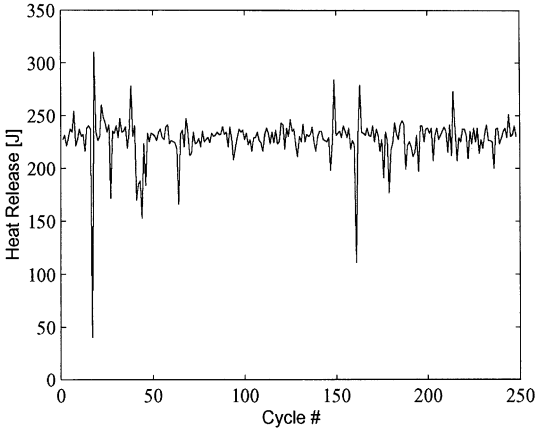


Fig. 7. Heat release for 248 consecutive cycles at AFR = 18.1. The plot clearly indicates incomplete combustion for several cycles. The estimated AFR for these cycles is 25.3.

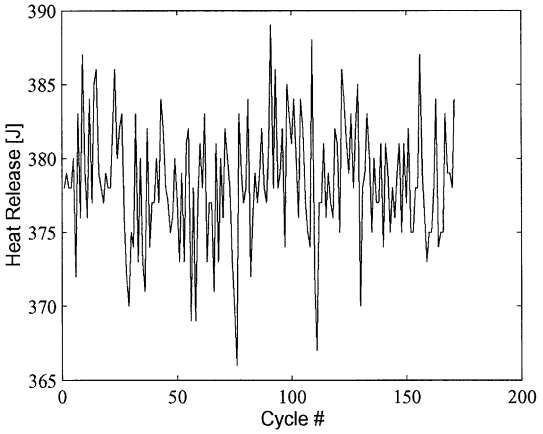


Fig. 8. Heat release for 171 consecutive cycles at AFR = 14.76. Compared to Fig. 7 the heat release is almost constant from cycle to cycle, indicating that combustion is nearly complete.

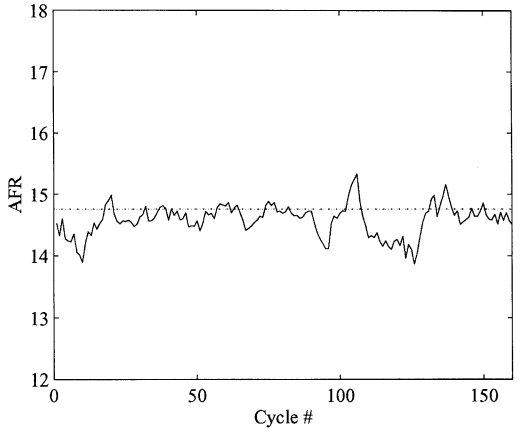


Fig. 9. Ten cycle moving average of AFR estimate. Steady-state operation with stoichiometric AFR.

that combustion is incomplete for a significant number of cycles. It is interesting to note that cycles with very high values of heat release follow immediately after cycles with incomplete combustion. This indicates that the residual gas (the gas which stays in the cylinder from one cycle to the next) contains a significant amount of unburned fuel. This is further evidence that the combustion of the preceding cycle was in fact incomplete. For reference, Fig. 8 shows the heat release for 171 consecutive cycles with an air/fuel ratio of 14.76. For these cycles the heat release is almost constant from cycle to cycle.

Fig. 9 shows a ten-cycle moving average of the AFR estimate for a steady-state experiment at stoichiometric operation (AFR = 14.7). The figure shows that most of the variance in the raw estimate is removed by taking the average over ten consecutive cycles.

## 7. Conclusion

The proposed model for estimating the AFR from cylinder pressure data performs well when cycle-averaging is performed. The RMS error of the AFR estimates from the validation data is 4.1%, which is somewhat better than with the molar weight ratio method proposed in Patrick (1989).

A drawback with the proposed estimator is that the variance of the estimates is large. The observed cycle-cycle variability is of such a magnitude that it cannot reflect actual variations in the cylinder AFR. The extremely simple turbulence model, used for the turbulent flame speed expression (8), which assumes that the turbulence intensity is completely determined by the engine speed, is a likely source of error.

An additional source of error is the assumption of a constant time derivative of the enflamed volume (11). As indicated in Section 4.1, the derivative of the enflamed volume depends on where in the combustion chamber

the flame center is located. Even though the flame is initiated in the spark-plug gap, the center of the flame may move away due to the in-cylinder flow field. This will result in a different expression for the enflamed volume derivative. Thus, since the flow field differs from cycle to cycle, the burn rate will also differ from cycle to cycle, and the burn rate is the basis for the AFR estimate.

The temperature dependence in the estimation model has not been verified in this work. Investigating this dependence would require a setup where the temperature of the intake air as well as the temperature of the coolant can be controlled.

The large variation from cycle to cycle of the cylinder-AFR estimate can be reduced by applying a low-pass filter or a moving average filter to the raw estimate. This will however lower the bandwidth of the estimator.

## 8. Discussion about applications

### 8.1. Cold start control

About 80% of the unburned hydrocarbons emitted from automotive engines today are produced during the cold-start phase. The cold-start phase is defined as the first 120 min of operation, before the catalytic converter has reached maximum conversion efficiency. During cold start, additional fuel has to be supplied, in order to compensate for poor fuel vaporization caused by condensation of fuel on cold surfaces.

In the present engine control systems, fuel is supplied according to an open-loop strategy during cold start, since the exhaust is too cold for the exhaust oxygen sensor to produce measurements. The open-loop strategies use a fuel correction factor which depends on the engine coolant temperature, in order to supply more fuel when the engine is cold. This means that deviations in the fuel delivery rates from fuel injectors compared to commanded fuel delivery rates will be directly reflected in errors in the cylinder AFR. In the case of too much fuel delivery, this means increased fuel consumption and hydrocarbon emissions. On the other hand, in the case of too little fuel delivery, rough engine operation and/or misfiring would result, also causing increased hydrocarbon emissions.

The proposed estimator can be used during coldstart while the exhaust gas is still too cold for the exhaust gas oxygen sensor to provide feedback. This would allow for closed-loop AFR control even during cold start. The high estimation variance is less of a problem during cold-start, since the cold-start phase consists mainly of idling, which implies nearly steady-state conditions. Thus, bandwidth is not a main concern, and the estimate can be low-pass filtered. The fact that the AFR estimator overestimates the AFR at the lean-limit, can be accounted for in a feedback control law with sensor saturation.

The objective of closed-loop control of AFR during cold start is more complicated than during warmed-up conditions. During warmed-up conditions the AFR dependence of the conversion efficiency of the catalytic converter dictates that the AFR be kept in a narrow band about 14.7, in order for both oxidizing and reducing reactions to take place. During cold start, the objective of the closed-loop control should be to minimize the total amount of hydrocarbons emitted during the whole cold-start phase. It is not completely understood today how to achieve this optimum. The difficulty here is that the tail-pipe emissions depend on both the raw emissions from the engine, and on the state of the catalytic converter. Furthermore, the state of the catalytic converter is affected by the exhaust that comes out of the engine.

To illustrate the complexity of the problem, two extreme cases can be considered. The first one is to keep the AFR during cold start at the level which minimizes the raw hydrocarbon emissions from the engine. Minimizing the raw hydrocarbon emissions from the engine will however slow down the heating of the catalytic converter, both through colder engine exhaust, and through less catalytic activity in the catalytic converter. The other extreme is to operate the engine rich during cold start, in order to minimize the time it takes for the catalytic converter to heat up to its normal operating temperature. This will produce high outputs of hydrocarbons during the initial stage of the cold start before the catalytic converter is hot, but allows faster transition to the normal stoichiometric operation of the engine, with high catalytic conversion efficiency. The optimum will be a trade-off between these two extremes, and will dictate a cold-start AFR trajectory which sacrifices some raw engine emissions in order to allow for faster heating of the catalytic converter, and consequently earlier transition to normal stoichiometric operation with high catalytic conversion efficiency.

### 8.2. Individual cylinder control

The proposed estimation technique is also valuable for estimating cylinder-specific AFR, which cannot be extracted from an exhaust gas oxygen sensor located in the exhaust manifold, where the exhaust from several cylinders is mixed. The intention is that the fuel and air delivery should be the same for all cylinders. In reality though, the difference in intake geometry for different cylinders cause differences in the air-flow rates through the intake ports. Also manufacturing tolerances and wear of fuel injectors can cause differences in fuel delivery characteristics between fuel injectors. For these reasons, the AFR may vary from cylinder to cylinder, which will result in different mechanical and thermal load on the different cylinders, as well as increased fuel

consumption and exhaust emissions, and reduced mechanical power output.

Estimating cylinder-specific AFR using the proposed method, allows control of the AFR on all cylinders individually. One way to implement this is to use the existing oxygen sensor for overall engine AFR control using some existing method, and use the individual cylinder AFR estimates to balance out the differences between the cylinders. This could be done by adding an integral term to the fuel delivery to cylinder $i$ of the form

$$\int_0^t [(k-1)\,\mathrm{AFR}_i - \mathrm{AFR}_{j,1} - \cdots - \mathrm{AFR}_{j,(k-1)}]\,\mathrm{d}t, \quad (29)$$

where $k$ is the total number of cylinders and $\mathrm{AFR}_{j,1}, \ldots, \mathrm{AFR}_{j,(k-1)}$ represent the individual AFR estimates of the other cylinders. This should, in steady-state, equalize the AFR estimates for all cylinders. Here, by making the gain of the integral term small enough, the influence of the estimate variance can be made arbitrarily small.

## References


Brunt, M. F. J., & Emtage, A. L. (1996). *Evaluation of IMEP routines and analysis errors*. SAE Technical Paper 97069.

Groff, E. G., & Matekunas, F. A. (1980). *The nature of turbulent flame propagation in a homogeneous spark-ignited engine*. SAE Technical Paper 800133.

Heywood, J. B. (1988). *Internal combustion engine fundamentals*. New York: McGraw-Hill, ISBN 0-07-100499-8.

Hires, S. D., Tabaczynski, R. J., & Novak, J. M. (1978). *The prediction of ignition delay and combustion intervals for a homogeneous charge, spark ignition engine*. SAE Transactions 87, SAE Technical Paper 780232.

Johansson, R. (1993). *System modeling and identification, Prentice-Hall information and system sciences series*. Englewood Cliffs, NJ: Prentice-Hall.

Metgalchi, M., & Keck, J. C. (1982). Burning velocities of mixtures of air with methanol, iso-octane, and idolene at high pressure and temperature. *Combustion Flame*, *48*, 191–210.

Patrick, R. S. (1989). *Air:fuel ratio estimation in an otto cycle engine: two methods and their performance*. Ph.D. thesis, Stanford University, Mechanical Engineering Department.

Pestana, G. W. (1989). *Engine control methods using combustion pressure feedback*. SAE Technical Paper 890758.

Powell, J. D. (1993). Engine control using cylinder pressure—past, present, and future. *Journal of Dynamic Systems Measurement and Control—Transactions of the ASME*, *115*(2B), 343–350.

Tunestål, P. (2000). *The use of cylinder pressure for estimation of the in-cylinder air/fuel ratio of an internal combustion engine*. Ph.D. thesis, University of California, Berkeley.

Tunestål, P., Wilcutts, M., Lee, A. T., & Hedrick, J. K. (1999). In-cylinder measurement for engine cold-start control. *Proceedings of the 1999 IEEE international conference on control applications*, Kona, Hawaii.

Tunestål, P., Lee, A. T., Wilcutts, M., & Hedrick, J. K. (2000). Lean-limit control of a spark ignition engine using IMEP-based incomplete combustion detection. *Proceedings of the advanced vehicle and engine control conference*, Ann-Arbor, Michigan.

Wibberley, P., & Clark, C. (1989). *An investigation of cylinder pressure as feedback for control of internal combustion engines*. SAE Technical Paper 890396.